Holzforschung, Vol. 60, pp. 253–258, 2006 • Copyright © by Walter de Gruyter • Berlin • New York. DOI 10.1515/HF.2006.041

Calculation of the relative bonded area and scattering coefficient from sheet density and fibre shape

Warren J. Batchelor[1,*] and R. Paul Kibblewhite[2]

[1] Australian Pulp and Paper Institute, Monash University, Victoria, Australia

[2] ensis-Papro, Rotorua, New Zealand

*Corresponding author.
Australian Pulp and Paper Institute, P.O. Box 36, Monash University, Victoria 3800, Australia
E-mail: warren.batchelor@eng.monash.edu.au

Abstract

The fraction of the available fibre surface in a sheet that is bonded to other fibres is the relative bonded area (RBA), which is an important determinant of sheet mechanical properties. The main method for estimating RBA has been to extrapolate data for the light scattering coefficient as a function of tensile strength to zero tensile strength. This method can produce significant errors. In this paper, the light scattering coefficient, corrected for the total surface area of the fibres available for scattering, was plotted against sheet density, corrected for fibre shape. This was carried out for sheets made from several series of pulps, including single furnishes of long- and short-fibre bleached and unbleached pulps, as well as sheets made of blends of bleached long- and short-fibre pulps. The corrected scattering coefficient was inversely linearly correlated to the corrected density for each data set. A theory was developed to allow RBA calculation from the intercept and slope of the fitted line.

Keywords: blended furnish; bonded area; eucalypt; fibre cross-sectional shape; fibre packing; radiata pine; relative bonded area; scattering coefficient; sheet density; wet pressing.

Introduction

The relative bonded area (RBA) is the fraction of the total available fibre surface that is bonded and is an important factor in controlling paper strength. It is defined as $RBA=(A_t-A)/A_t$, where A_t is the total area available for bonding and A is the unbonded area in the sheet after it has been formed. Two methods have been used to measure RBA: the nitrogen adsorption method (Brunauer et al. 1938) and the light scattering method (Ingmanson and Thode 1959). The light scattering method is more widely used, as it is much quicker. It assumes that $S=cA_s$, where S is the light scattering coefficient of a sheet, c is a constant that depends on the wavelength and the fibre properties and A_s is the surface area available for scattering. If S_0 is the scattering coefficient for a completely unbonded sheet, then $RBA=(S_0-S)/S_0$.

The major difficulty with the technique is in determining S_0, since an unbonded sheet cannot be prepared. Ingmanson and Thode (1959) plotted the scattering coefficient against tensile strength for sheets made from the same pulp. The sheet strength was varied by refining and/or wet pressing. The data were then fitted and extrapolated to determine the *y*-axis intercept at zero tensile strength, which was assumed to be S_0. One problem with this extrapolation is that the scattering coefficient-tensile curve found by these authors was non-linear, flattening out at very low strengths (Ingmanson and Thode 1959). The accuracy of the extrapolation depends on the lowest strength that can be obtained, which corresponds to an unrefined pulp and unpressed sheet. If, for the pulp being tested, the unrefined, unpressed sheets already have significant strength, the accuracy of the extrapolation is questionable. The original observation that all of the data from a single pulp fell onto one curve may also be a special case that is not generally applicable (Swanson and Steber 1959).

The problems of the extrapolation technique for determining S_0 were also recently highlighted with data from a series of sheets in which the fibre length was reduced by cutting the wet sheets before reslushing them and making handsheets (He et al. 2003b). The sheet strength decreased as the fibre length was reduced. Because of the reduction in sheet strength, the extrapolated value of S_0 decreased from 42.2 to 25.5 $m^2\ kg^{-1}$ as the fibre length was reduced from 3.14 to 1.80 mm (He et al. 2003b). The reduction in S_0 is not physically reasonable, as the cutting process would create new surfaces rather than reducing the area, providing further evidence that this extrapolation to determine S_0 cannot be correct. The extrapolation method is also completely unsuitable for measuring bonding in machine-made papers, since a range of sheets of different strengths cannot be obtained.

Recently one of the authors of this work published a paper showing that S is inversely linearly related to the apparent sheet density, ρ_a, provided the fibre shape is constant (Batchelor and He 2005). This could be true for sheets made from previously dried fibres, for which little change is typically observed in fibre cross-sectional dimensions with refining or wet pressing. This will not be true for sheets made from never-dried fibres, for which the fibre shape changes with wet pressing (He et al. 2003a). This observation explains differences in the literature, with both linear (El-Hosseiny and Abson 1979; Seth 1990b; Kibblewhite 1993; Paavilainen 1993; Iribarne and Schroeder 2000) and non-linear (Seth 1990a,b; Niskanen 1998) relationships reported between S and ρ_a.

The previous publication provided a method to correct S and ρ_a for fibre shape and showed that all the data could be fitted by a straight line when the corrected values were plotted against each other (Batchelor and He 2005). The equation for this line could then be used to

calculate RBA for any value of corrected apparent density. A limitation of this work is that the theory was only derived for single fibre furnishes and only tested on sheets made from fibres derived from a common starting stock of never-dried, unbleached radiata pine. The aim of this study was to extend the work by first modifying the theory for application to blends and then to test the theory against data measured for a wide range of sheets made from single and blended furnishes and softwood and hardwood fibres.

Theory

First a summary of the derivation of the original theory (Batchelor and He 2005) is presented. The derivation was for sheets made of one type of fibre only. Cross-sectional measurements (He et al. 2003a) have shown that the fibres largely lie flat in the sheet, with the fibre width, D_w, lying approximately parallel to the sheet surfaces. It was assumed that scattering arises from the widths of the fibres and that the lumen area does not contribute to scattering. The latter statement relies on the fact that two-thirds of the fibres in the sheet are either partially or fully collapsed (He et al. 2003a), even in low-density sheets made of unrefined, unbleached softwood kraft pulp. Under the assumptions described above, the total surface area available for scattering per unit mass of fibre was then $2D_w l/A_w\rho_w l$, where ρ_w is the fibre wall density, l is the fibre length and A_w is the fibre cross-sectional area. The total light scattering available from these fibres in the absence of bonding, which is S_0, was thus given by:

$$S_0 = c\frac{2D_w}{A_w\rho_w} \tag{1}$$

where c is a constant of proportionality. Eq (1) shows that S_0 is only constant provided that the fibre width and wall area are constant. It was next assumed that S is inversely linearly related to the apparent sheet density, ρ_a, provided that the fibre cross-sectional shape is constant. This inverse linear relationship was defined by two sets of points $(0,S_0)$ and (ρ_{max},S_{min}), where ρ_{max} is the maximum sheet density obtained when the fibres are perfectly closely packed. The corresponding scattering coefficient is S_{min}, which is not zero, because even when the fibres are perfectly closely packed, the irregular shape of the fibres means that they are not always in contact across their entire width. Light is scattered at the surfaces of the sheet and such a scattering surface is also included in S_{min}. Under these assumptions, S is related to ρ_a by:

$$S = S_0 - (S_0 - S_{min})\rho_a/\rho_{max}. \tag{2}$$

The maximum apparent density, ρ_{max}, will occur when all the fibres are lying flat, parallel and stacked perfectly on top of one another, such that there are no spaces between the bounding boxes surrounding the fibres. A fill factor, f, for a fibre was defined (see Figure 1) as the cross-sectional area of the fibre divided by the area, D_hD_w, of the smallest rectangular bounding box that can surround the irregular shape of the fibre (He et al. 2003a,b,c). The overall density of the bounding box is $f\rho_w$, where ρ_w is the density of the cell-wall material. By definition, then $\rho_{max} = f\rho_w$ and the ratio

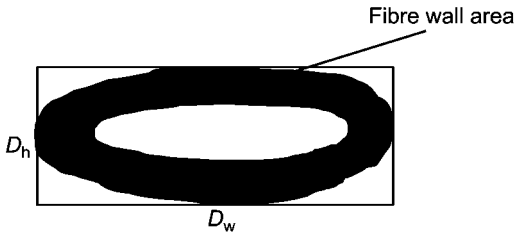

Figure 1 The bounding box surrounding a fibre cross-section.

$$\rho_a/f\rho_w \tag{3}$$

can be considered as the packing fraction of the sheet structure.

No theoretical expressions for S_{min} were available; rather, it was assumed that $S_{min} = rS_0$, where $r<1$ and r possibly depends on the pulp type, and certainly on grammage. Substitution into Eq. (2) of the expressions for S_0, S_{min} and ρ_{max} yielded:

$$S\frac{A_w\rho_w}{2D_w} = c - c\frac{\rho_a}{f\rho_w}(1-r). \tag{4}$$

For the work in this report, the theory above was extended to consider a sheet made from a blend of pulps. If the simplest case of a sheet made of a blend of two pulps is considered, labelled with subscripts 1 and 2, with mass fractions of m_1 and m_2, such that $m_1 + m_2 = 1$, then the total length of fibre fraction 1 in a unit mass of sheet is $m_1/A_{w1}\rho_w$. The total area per unit mass of sheet available for scattering from both fractions is $(2D_{w1}m_1/A_{w1}\rho_w) + (2D_{w2}m_2/A_{w2}\rho_w)$. Then the new form of Eq. (1) for a sheet made from two pulps is:

$$S_0 = (2c_1D_{w1}m_1A_{w2} + 2c_2D_{w2}m_2A_{w1})/A_{w1}A_{w2}\rho_w, \tag{5}$$

where c_1 and c_2 are constants of proportionality for the two pulps.

The maximum density is found by considering the blended sheet as consisting of two separate plies. The fractional packing of plies 1 and 2 is $\rho_a/f_1\rho_w$ and $\rho_a/f_2\rho_w$, respectively, and the packing fraction of the two-ply sheet structure, when averaged on a mass basis, is given by:

$$\frac{\rho_a}{\rho_w}\left(\frac{m_1}{f_1} + \frac{m_2}{f_2}\right). \tag{6}$$

By assuming that $c_1 = c_2$ and that r for the two pulps is the same, Eq. (4) can be rewritten as:

$$S\frac{A_{w1}A_{w2}\rho_w}{2D_{w1}m_1A_{w2} + 2D_{w2}m_2A_{w1}} = c - c\frac{\rho_a}{\rho_w}\left(\frac{m_1}{f_1} + \frac{m_2}{f_2}\right)(1-r). \tag{7}$$

Eq. (4) is then a simplified form of Eq. (7) for $m_2 = 0$.

The left-hand side of Eq. (7) is the scattering coefficient normalised by the total area available for scattering. In the remainder of the paper, this term is called the *normalised scattering coefficient*, while $(\rho_a/\rho_w)(m_1/f_1+m_2/f_2)$ is called the *fractional packing factor*, as it is the fraction of the sheet volume that is filled by the bounding boxes surrounding the irregular shape of the fibres. Eq. (7) implies that in plots of the normalised scattering coefficient vs. the fractional sheet density, all the points should lie on a straight line if the assumptions in the derivation are met. The validity of Eq. (7) is closely compared with the experimental data in the results section.

Finally, normalising Eq. (7) by c and substituting Eq. (5) yields:

$$\frac{S}{S_0}=1-\frac{\rho_a}{\rho_w}\left(\frac{m_1}{f_1}+\frac{m_2}{f_2}\right)(1-r), \tag{8}$$

which can be rearranged to yield:

$$\mathrm{RBA}=\frac{\rho_a}{\rho_w}\left(\frac{m_1}{f_1}+\frac{m_2}{f_2}\right)(1-r), \tag{9}$$

and thus RBA can be calculated from the sheet apparent density and the fibre shape for any single or blended furnish.

Material and methods

The data required by the theory are the sheet apparent density, the sheet scattering coefficient and the fibre shape parameters of fibre width, D_w, fibre thickness, D_h, and fibre wall area, A_w. The data used here were collected either at the Australian Pulp and Paper Institute (APPI) or at ensis-Papro in New Zealand. For both data sets, the dimensions of the fibres were characterised by measuring the wall area and by fitting a rectangular bounding box around each measured fibre and calculating the width, D_w, and height, D_h, of the bounding box. The fill factor was then calculated as $f=A_w/D_hD_w$. These dimensions are shown in Figure 1. The scattering coefficients were measured at 700 nm for the APPI data and at 557 nm for the ensis-Papro data. Sheet apparent density was measured using AS/NZS 1301.426 S: 1994. The major differences between the data sets lie in the sample preparation methods and analysis techniques that were used to measure the fibre cross-sectional dimensions. These differences are discussed and the data in each set are described.

APPI data (Batchelor and He 2005)

Samples were prepared from a single starting stock of an unbleached, laboratory-made, never-dried radiata pine kraft pulp, with a kappa number of 30. Different fractions were generated from the starting pulp by either hydrocyclone fractionation or cutting the fibres to reduce their length. The fibre dimensions were measured *in situ* in the sheet cross-sections that were embedded in resin and then exposed by polishing the resin-embedded blocks with abrasive paper (He et al. 2003a,b,c). A confocal microscope was used to visualise the fibres to avoid artefacts from surface preparation. The cross-sectional area of the fibres embedded in resin in the sheet was the same as for fibres separated from the sheet and dried onto glass slides, so it was concluded that the resin embedding process had not caused the dried fibres to swell (He et al. 2003c).

ensis-Papro data

Four sets of data from the literature were used. For each data set, the fibre dimensions were measured by embedding individual fibres in resin for optical microscopy using the method described by Kibblewhite and Bailey (1988). However, there were some differences in fibre preparation methods between the data sets and these are discussed.

e-P #1 Data for never-dried, unbleached radiata pine kraft pulps from different families and tree positions, as reported by Riddell et al. (2005) comprised data set e-P #1. The data were collected from two series of radiata pine clones and from two positions in each tree. From each sample, a kraft pulp with a kappa number of 30 was prepared and sheets were formed from the never-dried pulp. The handsheets were made from pulp refined for 500 rev in a PFI mill. Fibre shape was measured on fibres that had been rewetted from sheets made from unrefined pulp, before being dehydrated and embedded for microscopy and image analysis. These pulps were similar to the pulps used in the APPI data set.

e-P #2 New data were collected for two bleached softwood and one hardwood single pulps and blends of these pulps (Mansfield et al. 2004). The three pulps tested were a NIST standard eucalypt bleached pulp and two long-fibre reinforcement pulps, one predominantly spruce pulp from the Mackenzie mill in British Columbia, Canada and a radiata pine kraft pulp from the Tasman mill in New Zealand, labelled medium. Data were measured on sheets made from each of the individual furnishes and from long-fibre/short-fibre blends. Each pulp was supplied in dry-lap form.

Fibre shape and dimensions were measured by reslushing fibres from unrefined sheets made at only one pressing pressure. Because the fibre dimensions were measured on fibres from unrefined sheets, it was decided to use density and scattering coefficient data only from sheets with the lowest levels of refining, which were 500 and 1000 PFI rev for the softwood and hardwood pulps, respectively. This was to reduce the possibility that the shape measured for unrefined fibres could differ from the actual shape of the more heavily refined fibres in the sheet.

e-P #3 Historical data from Kibblewhite (1993) were used for three bleached softwood pulps and one hardwood pulp. These pulps included the eucalypt and Mackenzie pulps described above for e-P #2, as well as two radiata pine pulps labelled as low and medium standards. It should be noted that the medium radiata pine pulp in this set was not exactly the same as the medium pulp in e-P #2, as it was collected several years before the pulp in set e-P #2.

Unrefined fibres were prepared for measurement by dehydrating the fibres from a dilute slurry, followed by embedding for microscopy. Thus, the fibres that were measured for shape were never formed into sheets. This is in contrast to the sample preparation method for data sets e-P #1 and e-P #2. A large group of data is available from the e-P #3 data set, as refining was conducted at five specific levels of refining energy and three different SEL values for all four pulps; fibre shape, sheet density and light scattering were measured at all data points. The problem is that the fibres were prepared for shape measurement by solvent exchanging the wet-refined fibres. This process preserves the shape of the fibres after refining, but does not take into account the change in fibre shape when the sheet is formed. This is not an issue when fibres are prepared for testing by rewetting them from the sheet, since hornification ensures that, in the absence of significant mechanical treatment of the fibres, the fibres retain their shape from the sheet. For the e-P #3 data set, we only used data for unrefined sheets and for sheets made

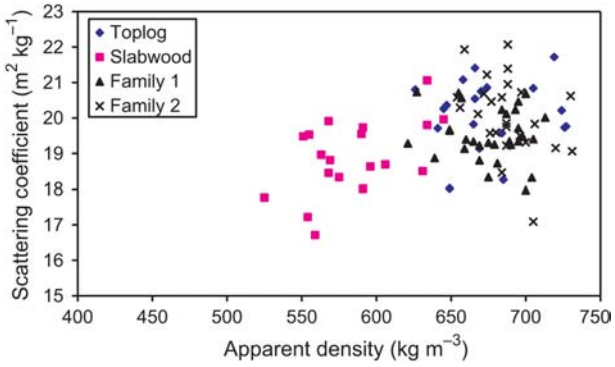

Figure 2 Scattering coefficient vs. sheet apparent density for the four data series from the e-P #1 data set.

after the lowest level of refining (40 kW h t^{-1}) to reduce errors from changes in fibre shape as the sheet was formed.

e-P #4 Historical data from Bawden and Kibblewhite (1997) comprised data set e-P #4. These were measured on a high-coarseness, unbleached radiata pine pulp from the Tasman mill in New Zealand. The study investigated the effect of multiple drying treatments with and without refining. Only the fibre shape data obtained by rewetting the fibres from the handsheets are used here to ensure that the fibre shape measured was similar to that in the sheet.

Results

To demonstrate the power of the new method, the e-P #1 data set is first discussed in detail. These data were taken from a number of individual trees and positions within the trees. Figure 2 shows the scattering coefficient, S, plotted against the sheet apparent density, ρ_a, for all 93 points. The data actually show a slight increase in S with increasing ρ_a, in complete contrast to the decrease with increasing ρ_a normally observed when a series of sheets from one pulp are tested. This trend arises because of differences in fibre wall area between the samples. A reduction in fibre wall area will make the sheet easier to consolidate, thus increasing the sheet density, given standard sheet-forming conditions. However, a decrease in fibre wall area will also increase the surface available for light scattering. Hence, it is possible

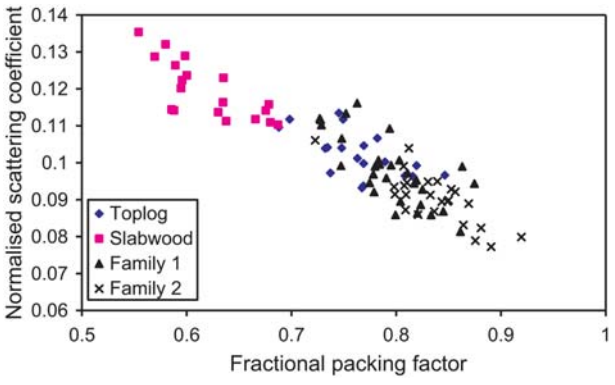

Figure 3 Normalised scattering coefficient vs. fractional packing factor for the different data sets that make up the e-P #1 series.

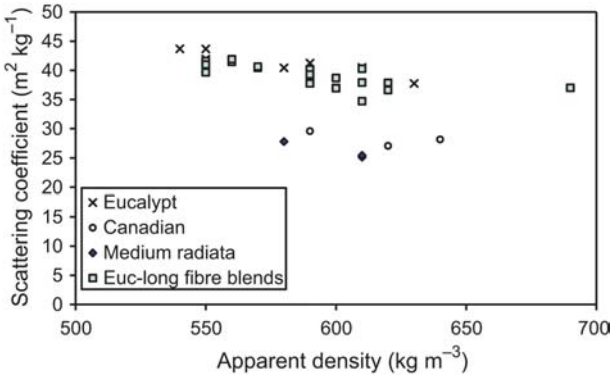

Figure 4 Scattering coefficient plotted against sheet apparent density for the ensis-Papro #2 data set.

to obtain an *increase* in S as ρ_a increases, provided that the increase in potential scattering surface outweighs the decrease in surface area from increased consolidation. However, even though the trend can be explained, Figure 2 is of no use in attempting to determine S_0 and RBA.

Figure 3 displays the normalised scattering coefficient plotted against the fractional packing factor for the e-P #1 set of data in Figure 2. The data from all series fall on a single line with negative slope, consistent with the theory. The data in Figure 3 also demonstrate the usefulness of this new theory in dealing with machine-made papers, where only the paper can be tested and the extrapolation according to Ingmanson and Thode (1959) cannot be applied.

In Figure 4, S is plotted against ρ_a for the e-P #2 data set. Sheets made from the eucalypt and eucalypt-long-fibre blends have considerably higher values of S than either the Canadian or medium radiata long-fibre furnishes. The eucalypt and eucalypt-long-fibre blend data appear to fall on a single straight line with negative slope. The normalised scattering coefficient is plotted against the fractional packing factor in Figure 5. The data show considerable scatter, but it appears likely that the data from all furnishes could be relatively well fitted by a single straight line. Certainly, the large differences in Figure 4 between the long- and short-fibre data have largely vanished in Figure 5 and the fact that the data fall approximately onto a single line with negative slope is again indicative of the usefulness of the method.

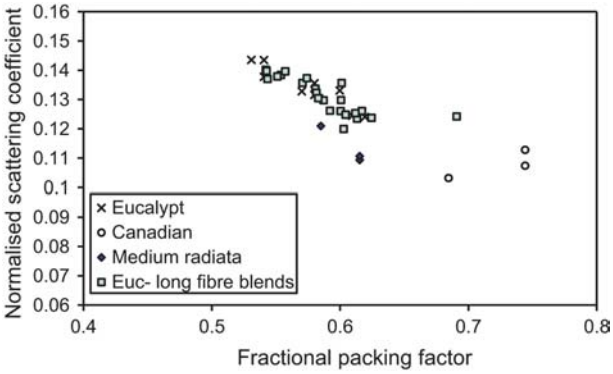

Figure 5 Normalised scattering coefficient plotted against fractional packing factor for the ensis-Papro #2 data set.

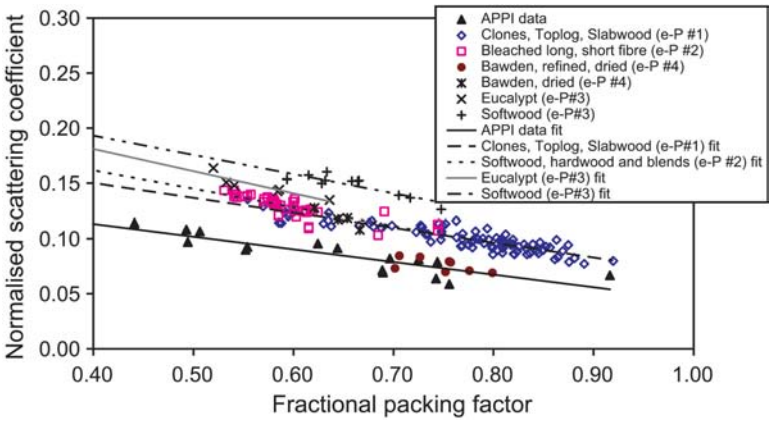

Figure 6 Complete data set of normalised scattering coefficient against fractional packing factor.

All of the data for the normalised scattering coefficient as a function of the fractional packing factor are plotted together in Figure 6. In this figure several of the data sets have been consolidated into one data series where it seemed likely that all of the data for a series fell on a single straight line. This is the case for the APPI data and the e-P #1 and #2. The historical refining data for e-P #3 seem to be split into two separate data series for the refined eucalypt pulp and the refined softwood pulps. After the data were consolidated into different series, a straight line was fitted through the data set and these fits are presented in Figure 6. e-P #4 seemed to be split into two groups. One group consists of sheets made from unrefined fibres that had been subjected to several drying treatments, while the second group consisted of sheets made from refined fibres that were then subjected to several drying treatments. The reason for the difference between the two groups of data points for the e-P #4 set is unclear at present.

Table 1 summarises the fits. The average values of $1–r$ is 0.71 and displays no trend for pulp type. The highest and lowest values were 0.77 (e-P #3 eucalypt) and 0.66 for the e-P #1 (unbleached softwood) and e-P #3 (bleached softwood pulps) sets, while the other two sets showed intermediate $1–r$ values of 0.72 and 0.73.

The assumption behind Eq. (7) is that scattering coefficient is negatively correlated to sheet density, provided that both can be corrected for changes in fibre shape. The data in Figure 6 and Table 1 fully support this assumption, as all of the data series were well fitted to a straight line. The worst fit produced an R^2 value of 0.68 (e-P #2), while all of the other fits were considerably better.

The APPI data set had the smallest intercept of 0.16, followed by the e-P #1 data set, with an intercept of 0.20, i.e., the data sets for unbleached pulps. The corresponding values for the bleached pulps from e-P #2, e-P #3 eucalypt and e-P #3 softwood were 0.23, 0.26 and 0.26, respectively. The intercept is the value of c, the constant of proportionality between the scattering coefficient and the surface area available for scattering in Eq. (7). This would be expected to be larger for a bleached pulp in comparison to an unbleached pulp, so the fits in Figure 6 agree with this expectation. It should not be automatically assumed that the fitted constants are applicable outside the data set for which they were measured. The value of $1–r$ gives the fraction of surface still available for scattering when the fractional packing factor is 1, and this may vary from furnish to furnish.

One surprise in the data was that the APPI data set is situated well below the e-P #1 data set, with a corresponding reduction in c, since both data sets were derived from sheets made from unbleached, never-dried radiata pine pulps with kappa 30. Some of the differences might be caused by the difference in wavelength used for the two sets of measurements: 700 nm for the APPI and 557 nm for the ensis-Papro data. The differences in fibre shape measurements between the two sets are described in detail in the materials and methods section, with *in situ* measurements used for the APPI data and ensis-Papro measurements made after reslushing and mounting. This difference also probably contributed to the discrepancy between the data sets.

A further surprise was the difference between the intercepts for e-P #2 data (sheets made from bleached eucalypt and softwood pulps) and the two e-P #3 series (also made from pulps of bleached eucalypt and bleached softwood). To investigate the source of this discrepancy, the scattering coefficient is plotted against sheet density for the NIST standard eucalypt pulp (e-P #2 and #3) in Figure 7. This figure shows that the data sets have approximately the same slope, but the more recent data

Table 1 Summary of the fits shown in Figure 6.

Sample group	No. of datapoints	R^2	Intercept	$1–r$
APPI data	21	0.88	0.16	0.72
e-P #1	92	0.82	0.20	0.66
e-P #2	39	0.68	0.23	0.73
e-P #3 eucalypt	6	0.82	0.26	0.77
e-P #3 softwood	18	0.76	0.26	0.66

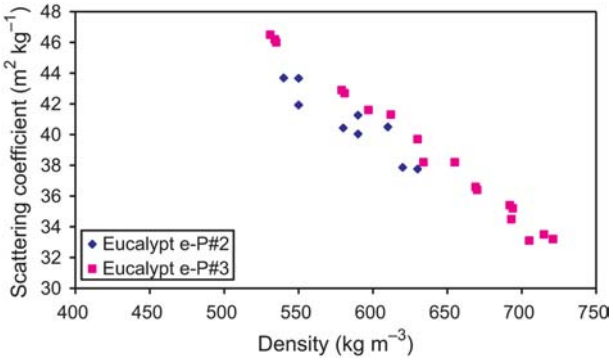

Figure 7 Relationship between two sets of data of scattering coefficient and sheet density for sheets made from NIST standard eucalypt pulp.

set (e-P #2) has a scattering coefficient ~2 $m^2 kg^{-1}$ lower than for the older data set (e-P #3) at the same sheet apparent density. The difference between the two curves in Figure 7 is therefore due to a real drop in the light scattering capacity of pulps between the earlier and later sets of measurements. Pulp ageing could be the reason for this observation.

Conclusions

Two new terms have been defined in this paper. The scattering coefficient corrected for the total surface area of fibres available for scattering is called the normalised scattering coefficient. The second term is the fractional packing factor, which describes the fraction of the paper structure filled by the bounding box around each approximately rectangular fibre. In this paper, previous work has been extended to allow the calculation of the normalised scattering coefficient and the fractional packing factor for sheets made of both single and blended furnishes. To calculate these parameters, it is necessary to measure fibre cross-sectional dimensions, as well as the scattering coefficient and sheet density.

The normalised scattering coefficient was found to be inversely correlated to the fractional packing factor, with a negative slope for sheets made from a wide range of bleached and unbleached pulps, as well as hardwood and softwood. The intercept and slope of the fitted line can be used to calculate the fraction of the available fibre surface that is bonded to other fibres – a quantity known as the RBA – which is an important determinant of the mechanical properties of sheets. RBA can now be calculated from one point alone without the need for extrapolation, which is inaccurate.

Acknowledgements

The analysis in this paper pulls together data from a number of our previously separately published papers. We would like to acknowledge our collaborators in these publications for their work. Funding from the Australian Research Council is also acknowledged.

References

Batchelor, W.J., He, J. (2005) A new method for determining the relative bonded area. Tappi J. 4:23–28.

Bawden, A.D., Kibblewhite, R.P. (1997) Effects of multiple drying treatments on kraft fibre walls. J. Pulp Pap. Sci. 23: J340–J346.

Brunauer, S., Emmett, P.H., Teller, E. (1938) Adsorption of gases in multimolecular layers. J. Am. Chem. Soc. 60:309–319.

El-Hosseiny, D.H., Abson, D. (1979) Light scattering and sheet density. Tappi 62:127–129.

He, J., Batchelor, W.J., Johnston, R. (2003a) The behaviour of fibers in wet pressing. Tappi J. 2:27–31.

He, J., Batchelor, W.J., Johnston, R.E. (2003b) An analytical model for number of fibre-fibre contacts in paper and expressions for relative bonded area (RBA). In: Proceedings of the 2003 International Paper Physics Conference, Victoria, Canada. Paptac. pp. 77–83.

He, J., Batchelor, W.J., Markowski, R., Johnston, R.E. (2003c) A new approach for quantitative analysis of paper structure at the fibre level. Appita J. 56:366–370.

Ingmanson, W.L., Thode, E.F. (1959) Factors contributing to the strength of a sheet of paper. Tappi 42:83–93.

Iribarne, J., Schroeder, L.R. (2000) The use of fundamental fiber properties to study pulp strength. In: Progress in Paper Physics – A Seminar, Grenoble, France, Vol. 2. EFPG Ecole Francaise de Papeterie et des Industries Graphiques. pp. 39–56.

Kibblewhite, R.P. (1993) Effects of refined softwood:eucalypt pulp mixtures on paper properties. In: Products of Papermaking: Transactions of the 10th Fundamental Research Symposium. Ed. Baker, C.F. PIRA International, Leatherhead, UK. pp. 127–157.

Kibblewhite, R.P., Bailey, D.G. (1988) Measurement of fibre cross-section dimensions using image processing. Appita J. 41:297–303.

Mansfield, S.D., Kibblewhite, R.P., Riddell, M.J.C. (2004) Characterization of the reinforcement potential of different softwood kraft fibers in softwood/hardwood pulp mixtures. Wood Fiber Sci. 36:344–358.

Niskanen, K. Paper Physics. Fapet Oy, Helsinki, 1998.

Paavilainen, L. (1993) Importance of cross-dimensional fibre properties and coarseness for the characterisation of softwood sulphate pulp. Pap. Puu 75:343–351.

Riddell, M.J.C., Kibblewhite, R.P., Shelbourne, C.J.A. (2005) Clonal variation in wood, chemical, and kraft fibre and handsheet properties of slabwood and toplogs in 27-year-old radiata pine. Appita J. 58:149–155.

Seth, R.S. (1990a) Fibre quality factors in papermaking I. The importance of fibre length and strength. In: Materials Interactions Relevant to the Pulp, Paper, and Wood Industries. Eds. Caulfield, D.F., Passaretti, J.D., Sobczynski, S.F. Materials Research Society, San Francisco, CA. pp. 125–141.

Seth, R.S. (1990b) Fibre quality factors in papermaking II. The importance of fibre coarseness. In: Materials Interactions Relevant to the Pulp, Paper, and Wood Industries. Eds. Caulfield, D.F., Passaretti, J.D., Sobczynski, S.F. Materials Research Society, San Francisco, CA. pp. 143–161.

Swanson, J.W., Steber, A.J. (1959) Fiber surface area and bonded area. Tappi 42:989–994.

Received December 4, 2005. Accepted February 22, 2006.